Preprints of the 19th World Congress
The International Federation of Automatic Control
Cape Town, South Africa. August 24-29, 2014

Gap Metric Bound Construction From Frequency Response Data

B. Ll. Jones *

* *Department of Automatic Control and Systems Engineering, The University of Sheffield, S1 3JD, UK (e-mail: b.l.jones@sheffield.ac.uk).*

Abstract: Motivated by the difficulty of designing low-order controllers for large-scale plants consisting of numerous interconnected subsystems, this paper addresses the issue of quantifying the ν-gap metric between the plant and a lower-order identified model, using only plant frequency response data. The main result of this paper is the construction of a bound on the ν-gap metric between plant and model that exploits the convergence properties of Chebyshev polynomial interpolants of point-wise in frequency system graph symbols. This bound subsequently informs the design of low-order robust controllers synthesised from the identified model. The techniques developed in this paper are demonstrated upon a semi-discretised 1D heat equation.

Keywords: Frequency response methods, Polynomial methods, Model approximation, Large-scale systems, Robust control.

1. NOTATION

In this paper $\mathbb{Z}$, $\mathbb{R}$ and $\mathbb{C}$ denote the natural, real and complex fields, respectively, and $s \in \mathbb{C}$ is a complex variable. The systems considered in this paper are linear and time-invariant (LTI) with the following state-space realisation:

$$\dot{x}(t) = Ax(t) + Bu(t), \tag{1a}$$
$$y(t) = Cx(t) + Du(t), \tag{1b}$$

where $A \in \mathbb{R}^{r\times r}$, $B \in \mathbb{R}^{r\times m}$, $C \in \mathbb{R}^{p\times r}$, $D \in \mathbb{R}^{p\times m}$, $x(t) \in \mathbb{R}^r$ is the state vector with initial state $x(0) = x_0$, $u(t) \in \mathbb{R}^m \subset \mathscr{L}_2[0,\infty)$ is the control input, $y(t) \in \mathbb{R}^p \subset \mathscr{L}_2[0,\infty)$ is the measurement and $\mathscr{L}_2[0,\infty)$ is the space of all signals of bounded energy. Taking the Laplace transform of (1) yields:

$$y(s) = P(s)u(s) = \left[C(sI-A)^{-1}B + D\right]u(s), \tag{2}$$

where I is the identity matrix and $P(s) \in \mathscr{R}^{p\times m}$ belongs to the space of proper real-rational transfer function matrices with p outputs and m inputs. The complex conjugate-transpose of $P(s)$ is denoted $P^*(s)$ and let $(\cdot\star\cdot)$ denote the Redheffer star product of two transfer function matrices with respect to some partition (Zhou and Doyle, 1998). Let $\mathscr{RL}_\infty$ denote the space of proper real-rational functions, bounded on $j\mathbb{R}$, and with norm $\|\cdot\|_\infty$, whilst $\mathscr{RH}_\infty$ is the space of proper real-rational functions that are bounded and analytic in the open right-half plane. The ordered pairs (N,M) and $(\tilde{N},\tilde{M})$ denote normalised right and left coprime factorisations of P, respectively, where $N,\tilde{N},M,\tilde{M} \in \mathscr{RH}_\infty$. Normalised right and left graph symbols for P are defined as $G := \left[\begin{smallmatrix} N \\ M \end{smallmatrix}\right]$ and $\tilde{G} := \left[\begin{smallmatrix} -\tilde{M} & \tilde{N} \end{smallmatrix}\right]$, respectively. The maximum singular value and determinant of a matrix are denoted $\bar{\sigma}(\cdot)$ and $\det(\cdot)$, respectively. The winding number of a scalar $g(s) \in \mathscr{RL}_\infty$ is denoted $\mathrm{wno}\, g(s)$ and is defined as the number of encirclements of the origin of $g(s)$, as s follows the standard Nyquist D-contour. With respect to computational complexity, the notation $f(q) \in O(h(q))$, where $q \in \mathbb{Z}$, means there exists $c \in \mathbb{R}_+$ and $q_0 \in \mathbb{Z}$ such that $|f(q)| \leq c|h(q)|$ for all $q > q_0$. Complexity is defined in terms of floating-point operations (flops), where a flop represents one addition, subtraction, multiplication or division of two floating-point numbers (Golub and Van Loan, 1996).

2. INTRODUCTION

The interconnection of numerous subsystems of low dynamical complexity can give rise to large-scale plants that display a dynamical wealth far in excess of their constituent parts. Examples include power fluctuations within distributed power grids (Zhong and Hornik, 2013), string instabilities in traffic systems (Swaroop and Hedrick, 1996) and congestion of the internet (Low et al., 2002). Such plants also arise from the discretization of systems governed by partial differential equations (PDEs), such as the flexing of beams, the propagation of sound, and the motion of fluid flows. Even when the plant dynamics are linear and time-invariant (or can be approximated as such), the problem of controlling them remains far from trivial.

A typical starting point to deriving a low-order controller assumes a model of a large-scale system in the form (1), wherein the state dimension is of the order of thousands or more. Low-order controllers can then be synthesised, either by performing model reduction and designing a controller from the resulting low-order model, or designing a large-scale controller and performing controller order reduction (Anderson and Liu., 1989). A variety of techniques have been developed to overcome the numerical difficulties associated with the model reduction of large-scale systems (Antoulas, 2005), such as Krylov subspace methods (Jaimoukha and Kasenally, 1994) and balanced proper orthogonal decomposition methods (Willcox and Peraire, 2002). However, such techniques typically seek low-order approximations that are close to the large-scale system in an open-loop sense, as measured by the difference in the $\mathscr{H}_\infty$-norm, for example. This can be problematic if the purpose of the low-order model is for feedback controller design, since the model reduction technique may neglect important closed-loop dynamics. For example, it was shown in Jonckheere et al. (1981) that models obtained from Hankel-norm model reduction may be unsuitable for robust controller synthesis owing to

perturbations vanishingly small in the Hankel norm leading to closed-loop instability.

For large-scale systems consisting of numerous smaller subsystems, alternatives to model/controller-reduction exist, wherein the structure of the subsystem interconnections can be exploited to efficiently derive feedback controllers. Such methods store only the models of the subsystems and so avoid any need for the explicit construction and storage of the system matrices of the large-scale plant. For the case of spatially invariant interconnected systems consisting of subsystems each with sensing and actuation capability, D'Andrea and Dullerud (2003) developed a state-space framework for designing distributed controllers. Conversely, if sensing and actuation is restricted to a small number of subsystems, then the design of a centralised controller is justified. An interesting example of centralised controller design for a spatially interconnected system was that of two-dimensional channel-flow with sensing and actuation restricted to discrete locations on the walls of the channel (Baramov et al., 2004). To overcome the high dimensionality of the underlying plant (of the order of 10^5), a model several orders of magnitude less than this was identified from frequency response data obtained not from simulation, but instead by exploiting the structure of the plant in an elegant fashion. This was achieved by computing the point-wise in frequency Redheffer star product of successive streamwise sections of the channel. Model validation techniques were then employed to establish the validity of the identified model. In a similar fashion, Dahan et al. (2012) identified a low-order model of the dynamics relating zero-net-mass-flux injection of a flow to pressure measurements on the rear of a three-dimensional backward facing step. Such geometries represent a simplified automobile, and are of interest for designing drag reduction systems to decrease fuel consumption. These authors obtained frequency response data via extensive numerical simulation of a system with state dimension on the order of 10^7. From this data, remarkably, a *second*-order transfer function was identified, from which a robust controller was synthesised which went on to successfully provide considerable drag reductions. However, such an approach does not provide an a priori guarantee that the controller, synthesised from the identified model, will robustly stabilise the actual plant. Attempts to reconcile such an issue, for example via worst-case identification in the ν-gap metric, were reported by Date and Vinnicombe (2004), and assumed a priori knowledge of a stabilising controller.

Motivated by these examples, this paper addresses the following question; given plant frequency response data, sampled at a finite number of frequencies, can a bound on the ν-gap metric between the plant and an identified model be constructed? The answer is affirmative and relies upon the rapid convergence of Chebyshev polynomial interpolants though the point-wise maximum singular values of $\mathscr{RL}_\infty$ functions. Assuming that the computation of the plant's frequency response is expensive, we detail a frequency refinement procedure for constructing the bound in a recursive fashion, starting from a small number of frequency samples, and provide guidelines for selecting an appropriate set of frequencies. We remark briefly that were $P(s)$ not large-scale then one would simply use the standard, $O(r^3)$ complexity, state-space formulae for computing the ν-gap (Vinnicombe, 2001).

The rest of this paper is organised as follows. Section 3 summarises the definitions and theorems required to state the main result of Section 4. Guidelines for the practical implementation

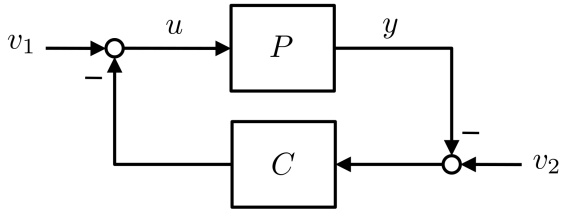

Fig. 1. Standard feedback interconnection.

of this result are also presented in Section 4, and these are applied to the numerical example of Section 5, followed by concluding remarks in Section 6.

3. PRELIMINARIES

With respect to Figure 1, let $[P,C]$ denote the standard feedback interconnection of plant $P \in \mathscr{R}$ and controller $C \in \mathscr{R}$. Define $[P,C]$ as stable provided the transfer function matrix in (3) belongs to $\mathscr{RH}_\infty$.

$$\begin{bmatrix} y \\ u \end{bmatrix} = \begin{bmatrix} P \\ I \end{bmatrix} (I - CP)^{-1} [-C \;\; I] \begin{bmatrix} v_2 \\ v_1 \end{bmatrix}. \tag{3}$$

The stability margin $b_{P,C}$ with respect to this arrangement is defined as:

$$b_{P,C} := \begin{cases} \left\| \begin{bmatrix} P \\ I \end{bmatrix} (I - CP)^{-1} [-C \;\; I] \right\|_\infty^{-1}, & \text{if } [P,\, C] \text{ is stable,} \\ 0, & \text{otherwise.} \end{cases} \tag{4}$$

The ν-gap metric between two plants $P_1,\ P_2 \in \mathscr{R}^{p\times m}$, denoted $\delta_\nu(P_1,P_2)$, is defined as (Vinnicombe, 2001):

$$\delta_\nu(P_1,P_2) := \begin{cases} \left\| \tilde{G}_2 G_1 \right\|_\infty, & \text{if } \det(G_2^* G_1)(j\omega) \neq 0 \; \forall \omega \in \mathbb{R} \\ & \text{and wno } \det(G_2^* G_1) = 0, \\ 1, & \text{otherwise,} \end{cases} \tag{5}$$

With respect to Chebyshev polynomial interpolation, the Chebyshev points $\{\psi_k\} \in [-1,1],\ \{k,n \in \mathbb{N} \mid 0 \leq k \leq n\}$, are defined as:

$$\psi_k := \cos(\pi k/n). \tag{6}$$

For a given number of points at which an interpolating polynomial is constructed, the following theorem establishes the error between such an interpolant and the underlying function.

Theorem 1. (Battles and Trefethen, 2004) Let $f(\cdot) : \mathbb{R} \to \mathbb{R}$ be a continuous function on $[-1,1]$, and $p_n(\cdot) : \mathbb{R} \to \mathbb{R}$ be its degree n polynomial interpolant in the Chebyshev points (6). If f has a d-th derivative in $[-1,1]$ of bounded variation for some $\{d \in \mathbb{N} \mid d \geq 1\}$, then:

$$\sup_\psi (f - p_n)(\psi) = O\left(n^{-d}\right) \text{ as } n \to \infty. \tag{7}$$

The interpolant is defined as $p_n(\psi) := \sum_{k=0}^n a_k T_k(\psi)$, where $\{a_k\}$ are the coefficients of the polynomial interpolant through the function values at the Chebyshev points $f(\psi_k)$, and the Chebyshev polynomials $T_k(\psi)$ are defined via the recursion $T_{k+1}(\psi) = 2\psi T_k(\psi) - T_{k-1}(\psi)$, with $T_0 := 1$ and $T_1(\psi) := \psi$ (Boyd, 2001). Chebyshev polynomial interpolants are employed in this work owing to their near-best properties for approximating smooth functions (Battles and Trefethen, 2004). Lastly, the following theorem provides a regularity result concerning the singular values of transfer function matrices.

Theorem 2. (Boyd and Balakrishnan, 1990) Let $H(s) \in \mathscr{RL}_\infty$ and suppose $\bar{\sigma}(H(j\omega))$ has a local maximum at $\omega = \omega_\mathrm{m}$. Then $\bar{\sigma}(H(j\omega_\mathrm{m}))$ is at least twice continuously differentiable.

These definitions and theorems are next applied to derive the main result of this paper.

4. ν-GAP BOUND CONSTRUCTION FROM FREQUENCY RESPONSE DATA

Given a set of frequency response data $\{P(j\omega_k)\}$ from some large-scale plant, we seek to compute $\delta_\nu(P,P_\mathrm{a})$, the ν-gap between this plant and a lower-order approximation P_a. Let P_n, $P_{a,n}$ denote the plant and model whose frequency responses are approximated by mapped Chebyshev interpolating polynomials at the following set of frequencies $\{\omega_k\} \in [0,\infty)$:

$$\omega_k = \gamma\frac{1+\psi_k}{1+\varepsilon-\psi_k}, \quad \leftrightarrow \quad \psi_k = \frac{\omega_k(1+\varepsilon)-\gamma}{\omega_k+\gamma}, \tag{8}$$

where $\{\gamma \in \mathbb{R} \mid \gamma > 0\}$ determines the frequency around which the $\{\omega_k\}$ are most densely distributed and $\{\varepsilon \in \mathbb{R} \mid \varepsilon > 0\}$ is vanishingly small. Such mappings enable Chebyshev polynomials interpolants, defined on the canonical domain $[-1,1]$ to be extended to functions on arbitrary domains (Boyd, 2001). We now state the main result.

Theorem 3. Given a plant $P \in \mathscr{R}^{p\times m}$, a set of $n+1$ Chebyshev points (6), data $\{P(j\omega_k)\}$ and a model $P_\mathrm{a} \in \mathscr{R}^{p\times m}$ such that wno $\det(G_\mathrm{a}^* G) = 0$, define $p_n(\psi)$ as the degree n polynomial interpolant of $f(\psi) := \bar{\sigma}\left(\tilde{G}_\mathrm{a} G\right)(j\omega(\psi))$ evaluated at the mapped points $\{\omega_k\}$ (8). Then there exists $\{\alpha \in \mathbb{R} \mid \alpha > 0\}$, $\{\beta \in \mathbb{N} \mid \beta \geq 3\}$ such that:

$$\delta_\nu(P,P_\mathrm{a}) \leq \sup_\psi p_n(\psi) + \alpha n^{-\beta} \text{ as } n \to \infty. \tag{9}$$

Proof. The proof proceeds from (5):

$$\begin{aligned}\delta_\nu(P,P_\mathrm{a}) - \delta_\nu(P_n,P_{\mathrm{a},n}) &= \sup_\omega \bar{\sigma}(\tilde{G}_\mathrm{a}G)(j\omega) - \sup_\omega \bar{\sigma}(\tilde{G}_{\mathrm{a},n}G_n)(j\omega),\\ &= \sup_\psi f(\psi) - \sup_\psi p_n(\psi),\\ &\leq \sup_\psi (f-p_n)(\psi).\end{aligned}$$

Next, note that $\tilde{G}_\mathrm{a}G \in \mathscr{RL}_\infty$ and so $\bar{\sigma}(\tilde{G}_\mathrm{a}G)(j\omega)$ is at least twice continuously differentiable, according to Theorem 2, and thus has a third derivative of bounded variation. The boundedness and continuity of the rational maps (8) and their derivatives ensures $f(\psi)$ also has a third derivative of bounded variation. Straightforward application of Theorem 1 completes the proof.

Thus, Theorem 3 provides a means of computing a bound on the ν-gap between plant and model, from frequency response data. Moreover, the convergence of the bound to the actual value of the ν-gap is rapid in the sense that the interpolation error decays *at least* as fast as $O(n^{-3})$. As an example to demonstrate such convergence, consider the following transfer function matrix $P(s) \in \mathscr{RL}_\infty$, where:

$$P(s) = \begin{bmatrix} P_0(s) & 0 \\ 0 & P_0(s^{-1}) \end{bmatrix}, \quad P_0(s) := \frac{\sqrt{3}s^2+\sqrt{2}s}{2s^2+2s+1}. \tag{10}$$

It can be shown that the highest derivative of bounded variation for $\bar{\sigma}(P(j\omega))$ is its third derivative (Boyd and Balakrishnan, 1990). For such a low-order system, it is possible to compute the Chebyshev polynomial interpolation error of $\bar{\sigma}(P(j\omega))$, as a function of interpolant order. This is plotted in Figure 2(b) on logarithmic axes, and clearly shows the error decaying with a slope of -3. Of course, if the plant is large-scale then it is not feasible to directly compute such an interpolation error. However, the parameters α and β governing the decay of the interpolation error can be obtained by considering the error

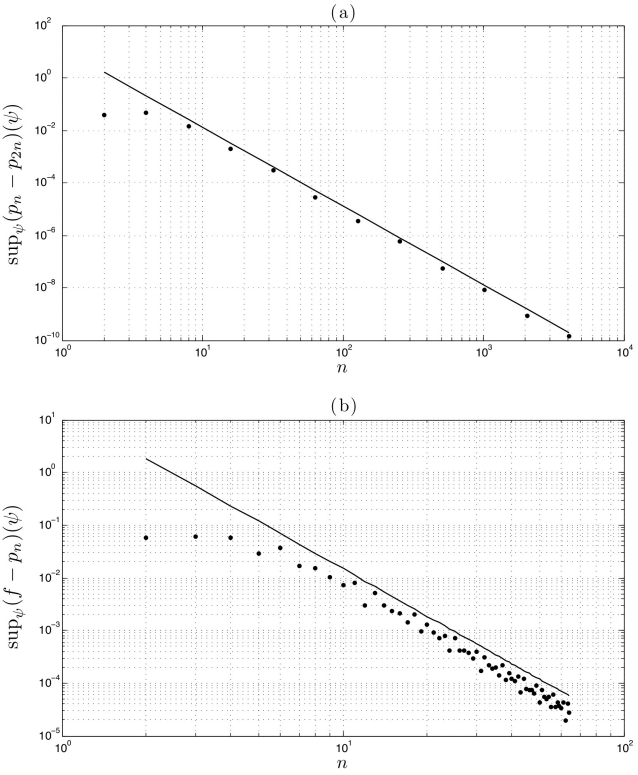

Fig. 2. Chebyshev polynomial interpolation of $P(j\omega)$ (10) showing (a) interpolation error between interpolants of degree n and $2n$ $(\cdot)$, plot of $\alpha(1-2^{-\beta})n^{-\beta}$ $(-)$, (b) actual interpolation error $(\cdot)$ and plot of $\alpha n^{-\beta}$ $(-)$. For this example, $\alpha = 14.9$, $\beta = 3$ and $\gamma = 0.6$.

between interpolants of different degrees, according to the following corollary.

Corollary 4. Assume $f(\psi)$ as defined in Theorem 3 and let $p_n(\psi)$, $p_{2n}(\psi)$ be its Chebyshev polynomial interpolants of degree $n, 2n$, respectively, then the following is true:

$$\alpha(1-2^{-\beta})n^{-\beta} \leq \sup_\psi (p_{2n}-p_n)(\psi) \text{ as } n \to \infty. \tag{11}$$

Proof.

$$\begin{aligned}\alpha(1-2^{-\beta})n^{-\beta} &= \alpha n^{-\beta} - \alpha(2n)^{-\beta},\\ &= \sup_\psi (f-p_n)(\psi) - \sup_\psi (f-p_{2n})(\psi) \text{ as } n \to \infty,\\ &\leq \sup_\psi \left((f-p_n)-(f-p_{2n})\right)(\psi) \text{ as } n \to \infty,\\ &= \sup_\psi (p_{2n}-p_n)(\psi) \text{ as } n \to \infty.\end{aligned}$$

Hence, bounds on α and β can be deduced from a logarithmic plot of the error between successive interpolating polynomials, and an example of this is shown in Figure 2(a). The following additional remarks are provided for guidance in computing the right hand side of (9).

Remark 5. The construction of, and subsequent operation upon interpolating polynomials is rendered straightforward by dedicated software, such as MATLAB's Chebfun toolbox (Battles and Trefethen, 2004).

Remark 6. Although the interpolation error decays rapidly ($\beta \geq 3$ in (9)) with increasing n, in the interests of efficient computation it is desirable to avoid evaluation of $\bar{\sigma}(\tilde{G}_{\mathrm{a},n}G_n)(j\omega)$ at an excessive number of interpolation points. With this in mind,

the convergence of the bound (9) with respect to the parameter α, is influenced by the choice of sampling frequencies $\{\omega_k\}$, determined by γ. The ideal choice is $\gamma = \omega_{\delta_\nu}$, where $\omega_{\delta_\nu} := \arg\sup_\omega \bar{\sigma}(\tilde{G}_a G)(j\omega)$, since this clusters the mapped Chebyshev points evenly around the frequency at which the ν-gap is achieved. Of course ω_{δ_ν} is not known a priori. However, a reasonable estimate can be obtained by observing that ω_{δ_ν} occurs in the vicinity of the open-loop crossover frequencies of the system singular values, which are typically known for controller design purposes. Furthermore, provided γ is within an order of magnitude of the ω_{δ_ν}, then the convergence of the interpolant is not adversely affected (Boyd, 2001).

Remark 7. Since the bound (9) is asymptotic, it is necessary to inspect convergence as the number of interpolation points increases. Selecting the order of the interpolant at each new iteration to be twice that of the previous iteration, as advocated in Corollary 4, ensures that the set of interpolation points for p_{2n} contains all the points used in forming p_n. Hence, the maximum number of function evaluations is not more than the smallest (power-of-two) n for which a given convergence tolerance is satisfied (Boyd, 2003).

A typical controller design procedure might proceed as follows:

(i) Select an approximate crossover frequency γ and evaluate $\{P(j\omega_k)\}$ at a small number $n_{\min}+1$ of mapped points (8).
(ii) Repeat step (i) at $2n+1$ interpolation points for $\{n \in \mathbb{N} \mid n_{\min} \le n \le n_{\max}\}$, until at $n = n_{\max}$ there is little change in the maximum singular value plots in the vicinity of the anticipated crossover frequency.
(iii) Identify a low order model $P_a(s)$ from the data $\{P(j\omega_k)\}$ and design pre/post-compensators, $W_1(s), W_2(s)$, respectively, to shape the singular value plots in a fashion consistent with design objectives. Construct the shaped model $P_{sa}(s) := W_2 P_a W_1(s)$ and synthesise the loop-shaping controller $C(s)$ that maximises the robust stability margin $b_{P_{sa},C}$ (4) (McFarlane and Glover, 1992). If $b_{P_{sa},C}$ is too small, then redesign the compensators until satisfactory robustness is achieved.
(iv) Shape the plant data to obtain $\{P_s(j\omega_k)\} := \{W_2 P W_1(j\omega_k)\}$ and compute $\{G_s(j\omega_k)\}$. From the low order model also compute $\{G_{sa}(j\omega_k)\}$ and use to verify the winding number criterion in (5).
(v) Evaluate $\{\bar{\sigma}(\tilde{G}_{sa} G_s)(j\omega_k)\}$ and compute the associated Chebyshev polynomial interpolant $p_{n_{\max}}(\psi)$ through these values.
(vi) Repeat step (v) for the values of n defined in step (ii) and apply Corollary 4 to obtain bounds on the interpolation error parameters α and β.
(vii) Set $n = n_{\max}$ and evaluate the right hand side of (9) from Theorem 3. Then check that the residual stability margin $b_{P_{sa},C} - (\sup_\psi p_n(\psi) + \alpha n^{-\beta})$ is acceptable.

An application of this procedure is demonstrated in the next section.

5. NUMERICAL EXAMPLE

Consider the following heat equation in a medium of one spatial dimension (Boskovic et al., 2001; Jones and Kerrigan, 2010) with a measurement of temperature gradient at one end:

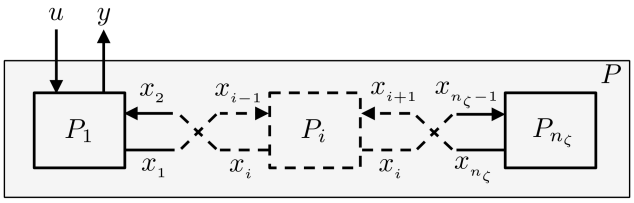

Fig. 3. Interconnection of grid-point models P_i forming the large-scale system P.

$$\frac{\partial \mathbf{x}(\zeta,t)}{\partial t} = \frac{\partial^2 \mathbf{x}(\zeta,t)}{\partial \zeta^2} + \lambda \mathbf{x}(\zeta,t), \quad \zeta \in \Omega, \tag{12a}$$

$$y(t) = \left.\frac{\partial \mathbf{x}(\zeta,t)}{\partial \zeta}\right|_{\zeta=-1}, \tag{12b}$$

with initial and boundary conditions:

$$\mathbf{x}(\zeta,0) = \mathbf{x}_0(\zeta), \tag{12c}$$

$$\frac{\partial \mathbf{x}}{\partial t}(-1,t) = \frac{-1}{\tau_u}\mathbf{x}(-1,t) + \frac{1}{\tau_u}u(t), \tag{12d}$$

$$\mathbf{x}(+1,t) = 0, \tag{12e}$$

where the temperature of the medium is $\mathbf{x}(\cdot,\cdot) : \Omega \times \mathbb{R}_+ \to \mathbb{R}$, and $\lambda = 2.39$ is a parameter that accounts for the internal heating of the material. $\Omega := [-1,1]$ is a bounded domain with left and right boundaries $\partial\Omega_{-1} = -1$ and $\partial\Omega_{+1} = 1$, respectively, $\zeta \in \Omega$ is a point within the domain and $y(\cdot) : \mathbb{R}_+ \to \mathbb{R}$ is the temperature gradient at the lower boundary. A control input $u(\cdot) : \mathbb{R}_+ \to \mathbb{R}$ is applied to a heating element with time constant $\tau_u = 1$ at the left boundary, whilst the right boundary satisfies the Dirichlet condition (12e) .

The system (12) is spatially discretised via second-order finite differences on a set of points $\{\zeta_1, \ldots, \zeta_{n_\zeta}\}$, where $\zeta_i := -1 + (i-1)\Delta_\zeta$ for $\{i \in \mathbb{N} \mid 1 \le i \le n_\zeta\}$, and the grid spacing $\Delta_\zeta := 2/(n_\zeta - 1)$ is constant. Under this approximation scheme, the state evolution at each interior grid point is given by:

$$\dot{x}_i(t) = \Delta_\zeta^{-2} x_{i-1}(t) + (\lambda - 2\Delta_\zeta^{-2}) x_i(t) + \Delta_\zeta^{-2} x_{i+1}(t), \tag{13}$$

with similar expressions for the boundary nodes. The inputs to each interior grid point model (13) are the states from neighbouring nodes, whilst the output is the state itself, thus defining the subsystem P_i. The interconnection between these subsystems is shown in Figure 3, from which it is apparent that the large-scale plant P is the chain of star products of each subsystem. In theory, a state-space realisation of P could be constructed in this way, with a state vector $x \in \mathbb{R}^{n_\zeta}$, but for fine discretisations ($n_\zeta = 1000$ in the present case) the resulting system matrices would be large and require significant storage. Instead, we proceed by computing the frequency response of the system in a point-wise fashion, by evaluating the star-product chain of subsystem frequency responses, according to the following expression:

$$P(j\omega) = P_1(j\omega) \star \ldots \star P_i(j\omega) \star \ldots \star P_{n_\zeta}(j\omega). \tag{14}$$

Given the small state-dimension of each subsystem, it can be shown for this example that the complexity of evaluating (14) is $O(n_\zeta)$ flops, as opposed to $O(n_\zeta^3)$ flops using standard LU factorisation (Golub and Van Loan, 1996) of the resolvent of $P(j\omega)$.

The design procedure of the previous section was applied as follows:

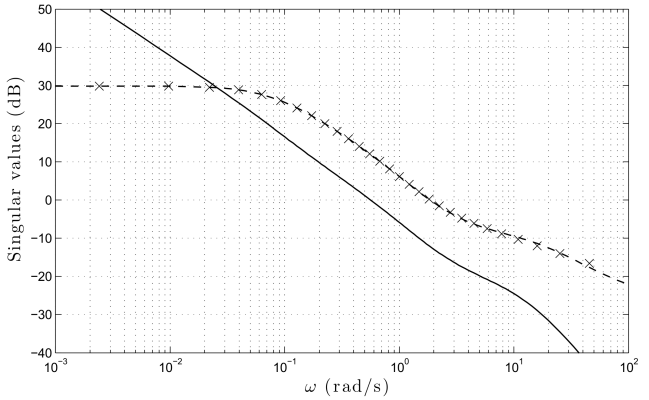

Fig. 4. Singular-values of plant data $\{P(j\omega_k)\}$ ($\times$), identified model $P_{\rm a}(j\omega)$ (——) and the shaped model $P_{\rm sa}(j\omega) := P_{\rm a}W_1(j\omega)$ (–).

(i) Anticipating the crossover frequency to be determined by the actuator dynamics (12d), a value of $\gamma = 1$ rad/s was selected and $\{P(j\omega_k)\}$ were evaluated at the set of points defined by (8), (6) with $n_{\min} = 2$.

(ii) The process was repeated for values of n up to $n_{\max} = 128$, whereupon little change around the anticipated crossover frequency was observed in the open-loop singular values $\{\bar{\sigma}(P(j\omega_k))\}$ at successive resolutions.

(iii) From the data $\{P(j\omega_k)\}$, a third-order model $P_{\rm a}(s)$ was identified using MATLAB's `fitsys` algorithm (Balas et al., 1998). Inspection of this model revealed a right-half plane zero at a frequency of $\omega \approx 1.8$ rad/s. To achieve a crossover frequency less than this, the following precompensator was used:

$$W_1(s) := \frac{10s+1}{4s(s+10)}; \tag{15}$$

Singular-value plots of $\{P(j\omega_k)\}$, $P_{\rm a}(j\omega)$ and the shaped model $P_{\rm sa}(j\omega)$ are shown in Figure 4. A $\mathscr{H}_\infty$ loop-shaping controller $C(s)$ was synthesised from the shaped plant, with a robust stability margin $b_{P_{\rm sa},C} = 0.52$.

(iv) The plant data was shaped to obtain $\{P_{\rm s}(j\omega_k)\} := \{PW_1(j\omega_k)\}$ from which the point-wise graph symbols $\{G_{\rm s}(j\omega_k)\}$ were computed. The point-wise graph symbols of the low-order model $\{G_{\rm sa}(j\omega_k)\}$ were also computed and used to form $\{\det(G^*_{\rm sa}G_{\rm s})(j\omega_k)\}$, the inspection of which revealed satisfaction of the winding number criteria (5).

(v) The set of values $\{\bar{\sigma}(\tilde{G}_{\rm sa}G_{\rm s})(j\omega_k)\}$ were computed, from which the Chebyshev polynomial interpolant $p_{n_{\max}}(\psi)$ was constructed. A plot of this interpolant as a function of frequency is shown in Figure 5, from which we obtain the first term on the right hand side of (9); $\sup_\psi p_{n_{\max}}(\psi) = 3.1 \times 10^{-3}$.

(vi) The interpolation error between successive interpolants $\sup_\psi(p_{2n} - p_n)(\psi)$ was evaluated for $n_{\min} \le n \le n_{\max}$ and plotted as in Figure 6. Inspection of the slope of this plot reveals an asymptotic order of convergence of order $O(n^{-3})$, hence $\beta = 3$. Corollary 4 was then applied to deduce $\alpha \le 1.14$.

(vii) Lastly, we apply (9) to obtain:

$$\begin{aligned}\delta_\nu(P_{\rm a}, P_{\rm sa}) &\le \sup_\psi p_{n_{\max}}(\psi) + \alpha n_{\max}^{-\beta},\\ &= 3.1 \times 10^{-3}.\end{aligned}$$

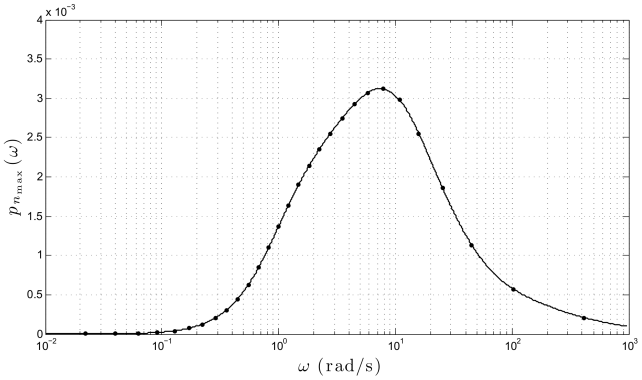

Fig. 5. Plot of the interpolating polynomial $p_{n_{\max}}$ (-) as a function of frequency ω through the interpolation points $\{\bar{\sigma}(\tilde{G}_{\rm sa}G_{\rm s})(j\omega_k)\}$ ($\cdot$).

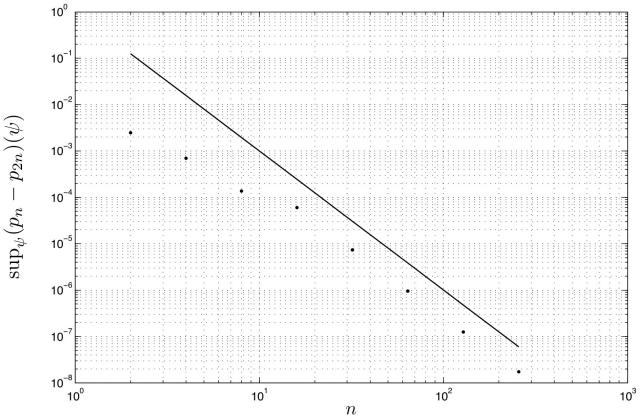

Fig. 6. Interpolation error between interpolants of degree n and $2n$ ($\cdot$), plot of $\alpha(1-2^{-\beta})n^{-\beta}$ ($-$) for $\alpha = 1.14, \beta = 3$.

We remark that the obtained bound on the ν-gap is negligible in comparison to the stability margin $b_{P_{\rm sa},C}$ and so we conclude that the controller $W_1C(s)$, obtained from the low-order identified model $P_{\rm a}(s)$, will robustly stabilise the plant $P(s)$.

6. CONCLUSION

The main contribution of this paper lay in the derivation of a bound on the ν-gap between a linear, time-invariant plant and a model identified from plant frequency response data. This is of particular relevance when the state-dimension of the underlying plant is too great to enable direct computation of the ν-gap, and where the plant possesses a structure that lends itself to efficient point-wise evaluation of its frequency response. This work therefore has application to the robust control of large-scale interconnected systems. Chebyshev polynomial interpolants were employed to construct the bound. By exploiting the smoothness of the maximum singular values of system graph symbols, together with the properties of Chebyshev polynomial interpolants, it was shown how the interpolation error decayed rapidly as a function of interpolant order. In practical terms this meant that relatively few frequency response evaluations were required to construct the bound, which subsequently informed the design of robust controllers synthesised from low-order identified models. Guidelines for the use of the bound were presented and demonstrated upon a semi-discretised 1D heat equation.

ACKNOWLEDGEMENTS

The author wishes to thank the reviewers of this paper for their valuable comments.

REFERENCES

Anderson, B.D.O. and Liu., Y. (1989). Controller reduction: concepts and approaches. *Automatic Control, IEEE Transactions on*, 34(8), 802–812.

Antoulas, A.C. (2005). An overview of approximation methods for large scale dynamical systems. *Annual Reviews in Control*, 29, 181–190.

Balas, G.A., Doyle, J.C., Glover, K., Packard, A., and Smnith, R. (1998). *μ-Analysis and Synthesis Toolbox for Use With* MATLAB*: User's Guide*. Mathworks Inc.

Baramov, L., Tutty, O., and Rogers, E. (2004). $\mathscr{H}_\infty$ control of nonperiodic two-dimensional channel flow. *Control Systems Technology, IEEE Transactions on*, 12(1), 111–122.

Battles, Z. and Trefethen, L.N. (2004). An extension of matlab to continuous functions and operators. *SIAM Journal on Scientific Computing*, 25(5), 1743–1770.

Boskovic, D.M., Krstic, M., and Liu, W. (2001). Boundary control of an unstable heat equation via measurement of domain-averaged temperature. *Automatic Control, IEEE Transactions on*, 46(12), 2022–2028.

Boyd, J.P. (2001). *Chebyshev and Fourier Spectral Methods*. Dover, Mineola, New York, 2 edition.

Boyd, J.P. (2003). Computing zeros on a real interval through chebyshev expansion and polynomial rootfinding. *SIAM Journal on Numerical Analysis*, 40(5), 1666–1682.

Boyd, S. and Balakrishnan, V. (1990). A regularity result for the singular values of a transfer matrix and a quadratically convergent algorithm for computing its $\mathscr{L}_\infty$-norm. *Systems & Control Letters*, 15(1), 1–7.

Dahan, J.A., Morgans, A., and Lardeau, S. (2012). Feedback control for form-drag reduction on a bluff body with a blunt trailing edge. *Journal of Fluid Mechanics*, 704, 360.

D'Andrea, R. and Dullerud, G. (2003). Distributed control design for spatially interconnected systems. *Automatic Control, IEEE Transactions on*, 48(9), 1478–1495.

Date, P. and Vinnicombe, G. (2004). Algorithms for worst case identification in h and in the ν-gap metric. *Automatica*, 40(6), 995–1002.

Golub, G.H. and Van Loan, C.F. (1996). *Matrix Computations*. The Johns Hopkins University Press, third edition.

Jaimoukha, I.M. and Kasenally, E.M. (1994). Krylov Subspace Methods for Solving Large Lyapunov Equations. *SIAM Journal on Numerical Analysis*, 31(1), 227–251.

Jonckheere, E.A., Safanov, M.G., and Silverman, L.M. (1981). Topology induced by the Hankel norm in the space of transfer matrices. In *Proc. 20th IEEE Conference on Decision and Control including the Symposium on Adaptive Processes*, volume 20, 118–119.

Jones, B.L. and Kerrigan, E.C. (2010). When is the discretization of a spatially distributed system good enough for control? *Automatica*, 46(9), 1462–1468.

Low, S.H., Paganini, F., and Doyle, J.C. (2002). Internet Congestion Control. *IEEE Control Systems*, 22(1), 28–43.

McFarlane, D. and Glover, K. (1992). A loop shaping design procedure using $\mathscr{H}_\infty$ synthesis. *Automatic Control, IEEE Transactions on*, 37(6), 759–769.

Swaroop, D. and Hedrick, J.K. (1996). String Stability of Interconnected Systems. *Automatic Control, IEEE Transactions on*, 41(3), 349–357.

Vinnicombe, G. (2001). *Uncertainty and Feedback*. Imperial College Press.

Willcox, K. and Peraire, J. (2002). Balanced model reduction via the proper orthogonal decomposition. *AIAA Journal*, 40(11).

Zhong, Q. and Hornik, T. (2013). *Control of Power Inverters in Renewable Energy and Smart Grid Integration*. Wiley-Blackwell.

Zhou, K. and Doyle, J.C. (1998). *Essentials of Robust Control*. Prentice Hall.